# Low-loss and high-$Q$ planar metamaterial with toroidal moment

Yuancheng Fan,[1,2,*] Zeyong Wei,[1] Hongqiang Li,[1,†] Hong Chen,[1] and Costas M. Soukoulis[2,3,‡]

[1]*Key Laboratory of Advanced Micro-structure Materials (MOE) and Department of Physics, Tongji University, Shanghai 200092, China*

[2]*Ames Laboratory and Department of Physics and Astronomy, Iowa State University, Ames, Iowa 50011, USA*

[3]*Institute of Electronic Structure and Laser, FORTH, 71110 Heraklion, Crete, Greece*

(Received 16 October 2012; revised manuscript received 15 January 2013; published 15 March 2013)

We experimentally observe toroidal dipolar response in a planar metamaterial comprised of asymmetric split-ring resonators (ASRRs) at microwave frequency. It is shown that a toroidal molecule can be constructed through rational arrangement of planar ASRRs as meta-atoms via manipulating structural symmetry and thus coupling of the meta-atoms. We find that the toroidal resonance provides a subwavelength-scale electromagnetic localization style, and that confining the electromagnetic field inside a dielectric medium with toroidal geometry is beneficial for low-loss metamaterials. The planar scheme of manipulating the coupling among the ASRRs may stimulate research in optical regions involving toroidal multipoles. The toroidal geometry together with the Fano resonance of ASRR-induced high-$Q$ response will have enormous potential applications in enhancing light-matter interactions, e.g., for low-threshold lasing, low-power nonlinear processing, and sensitive biosensing.

DOI: 10.1103/PhysRevB.87.115417 PACS number(s): 78.67.Pt, 41.20.Jb, 73.20.Mf, 74.25.N−

## I. INTRODUCTION

The toroidal moment is of fundamental interest in the physics community.[1] The toroidal response produced by currents flowing on the surface of a torus along its meridians was first considered by Zel'dovich to explain parity violation in the weak interaction.[2] The so-called anapoles[2] have gained acceptance in nuclear and particle physics.[3,4] Theoretical calculation has also predicted toroidal moments in special molecular[5] and ferroelectric[6] structures. Toroidal multipoles are different from electric dipoles produced by negative and positive charge or magnetic dipoles created by the current in the closed loop in traditional multipole expansions. Particularly, the nonradiating feature of the toroidal geometry is quite unique, which comes from poloidal currents flowing on the surface of a torus. The toroidal dipole points outward along the symmetry axis of the torus. So, suppressing traditional electric and magnetic multipoles and enhancing toroidal response by rationally manipulating structural symmetry are basic and essential towards providing the interesting optical phenomena associated with the toroidal dipolar moment.

Since there exists a profound analogy between the weak and the electromagnetic interactions, it is interesting to know whether we can reconstruct this unusual interaction in manipulating electromagnetic waves, which would have important implications in our modern life. Metamaterial[7] is simply a concept of artificially constructing microstructured materials with high-quality properties unattainable in nature; these artificial materials usually consist of subwavelength-sized metallic resonant building blocks as meta-atoms,[8] which yield electric or/and magnetic responses.[9,10] The local resonances of the meta-atoms and mutual coupling among them enable the manipulation of electromagnetic waves at a subwavelength scale.

Toroidal metamaterial was first theoretically proposed in investigating a three-dimensional (3D) array of toroidal solenoids,[11] later experimentally studied in a toroidal wiring consisting of four rectangular loops, its response analyzed in terms of multipole moments;[12] however, the toroidal moment is not dominant in the structure. It was found that toroidal metamaterials can make a negative index of refraction and rotate the polarization state of light.[11,12] In 2010 toroidal-dominated response in microwave regions was first experimentally demonstrated by three-dimensionally arranging four split-ring resonators (SRRs) in a unit cell of toroidal symmetry[13] and later theoretically scaling them[14] to far-infrared wavelengths. However, the 3D arrangements of four SRRs are difficult to fabricate at optical wavelengths with toroidal dipolar moments. Although there have been some attempts in manufacturing 3D SRR structures, it is a challenge not only at optical frequencies, but also at microwave frequencies.[13] Stacking of two-dimensional planar plasmonic metamaterial structures is assumed to be the pathway towards the third dimension in the optical regime. These metamaterials have exhibited exotic properties and potential applications: for artificial magnetic composites,[15] a perfect absorber,[16] and as an electromagnetically induced transparency medium.[17–21] The planar-structure-based scheme is not limited to microwave bandwidths but also shows good performance at terahertz bands[22] and even in the optical range.[23–25]

In this paper, we show a planar scheme for toroidal metamaterial, with the unit cell comprised of four asymmetric split-ring resonators (ASRRs). We demonstrate that a toroidal molecule can be constructed through arrangement of planar ASRRs as meta-atoms via manipulating structural symmetry among the meta-atoms. Field maps clearly indicate that the toroidal resonance paves fantastical electromagnetic field confinement in dielectric substrates within a subwavelength-sized volume of toroidal geometry. This planar scheme, by manipulating the coupling among the ASRRs, may stimulate research in optical regions involving toroidal multipoles. Toroidal geometry together with Fano resonance of the ASRR makes an even higher-$Q$ responsed metamaterial, in which light-matter interaction will be significantly amplified.[26] Planar toroidal metamaterial will have myriad potential applications with low Joule loss,[27] low-threshold plasmonic lasing,[28] low-power nonlinear processing,[29] and sensitive biosensing.[30]

 

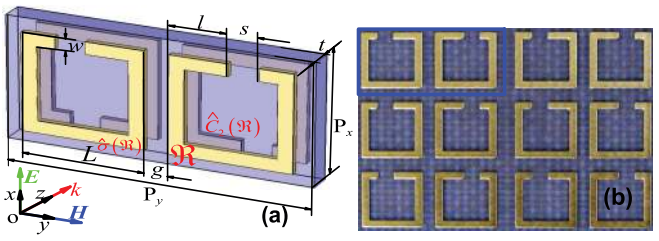


FIG. 1. (Color online) (a) Schematic of the unit cell for the ASRR-based planar toroidal metamaterial and corresponding electromagnetic excitation configuration (with polarization direction along the $x$ axis). (b) Photograph of the toroidal metamaterial slab; geometric parameters are denoted by black letters in Fig. 1(a).

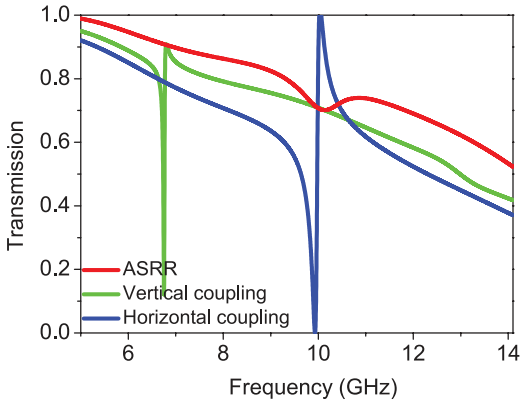


FIG. 2. (Color online) Comparison of spectra between single ASRR and ASRR pairs for investigating the coupling mechanism: FDTD calculated transmission spectra for planar metamaterial unit cell with only a single ASRR (red curve), a vertical coupled ASRR pair (green curve), and a horizontal coupled ASRR pair (blue curve).

## II. PLANAR TOROIDAL METAMATERIAL: THEORETICAL DISCUSSIONS AND EXPERIMENTAL RESULTS

The designed planar structure is comprised of two metallic layers and a dielectric spacer layer. A unit cell of our model slab or the toroidal molecule is shown stereographically in Fig. 1(a); the toroidal molecule is constructed through rational arrangement of four ASRRs as meta-atoms via manipulating the structural symmetry of the meta-atoms. Pairs of ASRRs in the same layers are of mirror symmetry about the $xz$ plane ($\sigma$), and pairs of ASRRs in the different layers are of 180° rotational symmetry about the $y$ axis ($C_2$). We note that throughout our study metamaterials are illuminated by $x$-polarized (electric field $\boldsymbol{E}$ is along the $x$ axis) electromagnetic waves both in experiments and calculations, as illustrated in Fig. 1(a).

The toroidal molecule in our model system is constructed from four contiguous ASRRs as meta-atoms. Since these meta-atoms are in close proximity, the nearest-neighbor mutual interactions or hybridizations[31–34] between them play a determinative role in their collaborative response to external excitations. We first investigate the response of a single ASRR and then mutual coupling interactions in pairs of the ASRRs. We performed all numerical calculations with a brute-force finite-difference-in-time-domain (FDTD)[35] electromagnetic solver (Gallop).[36] For a metamaterial with its unit cell being only one ASRR, it is shown that the *trapped mode* can be excited even under normal electromagnetic incidence conditions in a recent study;[37] the trapped mode originates from symmetry breaking to some extent of the metallic element of a metamaterial. Introduction of small structural asymmetry causes a degeneration from the *dark mode*[38] to the trapped mode, or we can say that a weakly coupled nature shifting to an external excitation of an ASRR is an inherited attribute from the dark mode. For the single ASRR unit-cell case, frequency plot performance of the transmission is shown as a red curve in Fig. 2. The dip position near 10 GHz indicates the trapped mode of ASRR. The resonant response appears to have Fano line shape[39–41] as a result of the destructive interference between the trapped sharp resonance and free space propagating in a continuumlike spectrum, which has shown its immense potential in ultrasensitive spectroscopy and/or biosensing applications.[30] In bringing ASRRs into the toroidal geometry, here we may get an even higher $Q$ response. Meanwhile, we noted that the single ASRR is of weak excitation, again verifying that the trapped mode of ASRR is weakly coupled to external excitation, since electromagnetic waves can easily leak through the unpatterned area of the metasurface.

Continuatively we consider coupling interactions between the ASRRs, since the mutual coupling is remarkable between closely spaced metallic particles,[31–34] and the coupling plays a crucial rule in formation of the toroidal mode. Numerical simulations were first carried out for the structure of an in-plane ASRR pair [i.e., $\Re$ and $\hat{\sigma}(\Re)$ in Fig. 1(a)] as the fundamental element. The transmittance spectrum is represented by the blue curve in Fig. 2, in which only one resonance is clearly observable. We call this kind of interaction horizontal coupling. The single peak response comes from in-plane mirror symmetry. Only the mirror symmetric surface current can be excited under normal incidence because the antisymmetric surface current cannot be excited, and since there is no phase retardation, the antisymmetric mode is now a dark mode.[38]

For the structure of a stacked ASRR pair [i.e., $\Re$ and $\hat{C}_2(\Re)$ in Fig. 1(a)] as the fundamental element, the transmittance spectrum is represented by the green curve in Fig. 2. There now exist two resonances: one strong (6.8 GHz) and one weak (12.9 GHz). We call this kind of interaction vertical coupling. The two resonances are far away from the original magnetic trapped mode (10 GHz) of ASRR, which is due to extreme overlap of the two magnetic trapped modes of ASRRs in the vertical coupling configuration. We also note that for the low-frequency mode magnetic oscillations of the ASRRs are in phase. This is crucial for toroidal response in our planar metamaterial system. The twofold rotational symmetry of the metamolecule caused the in-phase response at low frequency.

Finally, we construct a metamolecule involving the previously mentioned horizontal coupling and vertical coupling with four ASRRs for toroidal response. Figure 3 presents the FDTD calculated and experimentally measured transmission spectra. The calculated intensity of the transmitted wave (red solid curve) clearly shows two Fano-shaped resonances coming from the destructive interference between the

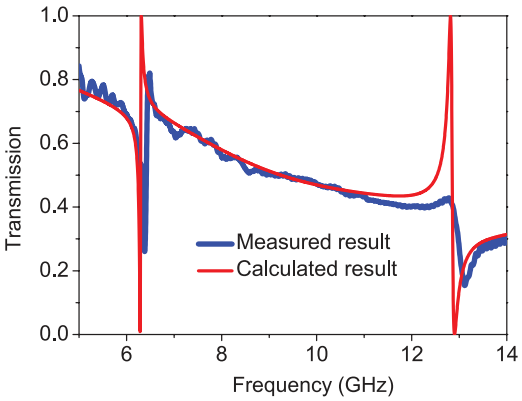


FIG. 3. (Color online) Experimentally measured (blue curve) and FDTD calculated (red curve) dispersion of transmitted power of the designed planar toroidal metamaterial.

collective sharp response of the meta-molecule and the free space propagating in the continuumlike spectrum.

The two resonances have their characteristic frequency nearly the same as the vertical coupled ASRR pair (green line in Fig. 2). The frequency of the higher resonance at 12.905 GHz (marked with the peak frequency) is determined by the out-of-phase vertical coupling. The higher resonance is clearly observable as in the color map of the $z$-component magnetic field in Fig. 4(b). Coupling in this manner causes a net nonzero magnetic component along the $y$ axis. Meanwhile, the frequency of the lower resonance at 6.378 GHz (marked with the peak frequency) is determined by the in-phase vertical coupling. The in-phase coupled magnetic mode [see color map of the $z$-component magnetic field in Fig. 4(a)] together with horizontal coupling under normal electromagnetic incidence made a circumfluent magnetic field or magnetic vortex. This is rightly a picture of the toroidal dipolar,[13] which shows a subwavelength electromagnetic localization within the dielectric substrate with a toroidal configuration.

We fabricated a sample with exactly the same parameters as our theoretical model. A printed circuit board (PCB) with metal sheets (0.035 mm thick) attached to both sides of a 0.787-mm-thick commercial Taconic TLX-8 dielectric substrate with permittivity $\epsilon_r = 2.55$ is employed for the sample fabrication. The metamolecule array has a lattice constant of $P_x = 5$ mm and $P_y = 10$ mm. The metal strip width is $w = 0.5$ mm wide, the outer width of the ASRRs is $L = 4$ mm, the inner gap between the two in-plane ASRRs is $g = 0.8$ mm, and a $s = 1$ mm wide split is opened on the original square ring with a distance $l = 1.9$ mm away from the central sideline. The overall lateral size of our planar metamaterial slab is 540 mm $\times$ 440 mm (54 $\times$ 88 unit cells). The transmission spectra through our sample were measured with a vector network analyzer Agilent 8722ES in an anechoic chamber. The measured results (blue solid curve in Fig. 3) meet quite well with the theoretical predictions. The two resonances of our model system are all clearly observable in the experimental spectrum. However, we found a curious and abnormal phenomenon: the low-$Q$ coupled magnetic resonance at high frequency is less obvious while the high-$Q$ toroidal resonance at low frequency is quite obvious. We believe that this is due to the exotic field localization configuration of the toroidal geometry. This can

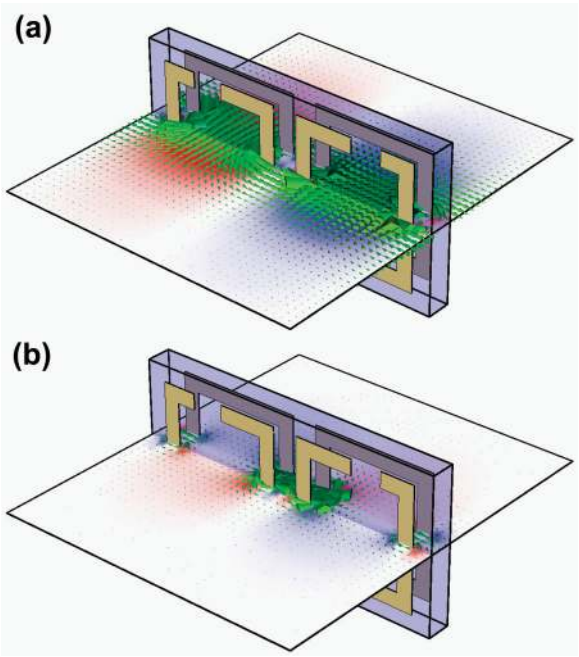


FIG. 4. (Color online) Calculated spatial distributions of vectorial magnetic field for correspondingly toroidal mode and magnetic mode plotted over the color maps of $z$-component magnetic field at peak frequencies 6.378 GHz (a) and 12.905 GHz (b), respectively.

be checked by looking at the evolution of the magnetic field inside the structure as calculating the spatial field distribution shown in Fig. 4. In the toroidal mode (at 6.378 GHz), most of the field is restricted to flowing inside the dielectric substrate, while for the coupled magnetic mode (at 12.905 GHz), the field is confined on the metal surface. A strongly enhanced field that is localized on metal surfaces causes amplified metallic absorption in the coupled magnetic mode (at 12.905 GHz) as in previous metamaterial structures. For toroidal mode the fields mainly distributed in the dielectric substrate within a subwavelength-sized volume of toroidal geometry, which is important for overcoming metallic losses in metamaterials. Planar toroidal metamaterials offer strikingly different qualities for the field of electromagnetics, exhibiting a convincing manifestation of the abnormal low-loss phenomenon of the toroidal mode. This finding of the toroidal geometry has benefits for low-Joule-loss metallic photonic metamaterials.[27]

Radiating power for induced multipole moments is calculated through integrating spatial distributed fields over the volume of the planar metamolecule with current density formalization.[13] Figure 5 shows the radiating power of three major multipoles of the planar metamaterial system: the electric dipole (blue dashed curve), the magnetic dipole (green dash-dotted curve), and the toroidal dipole (red solid curve). As can be seen from Fig. 5, the electric dipole $\boldsymbol{P}_x$ shows large components in the full frequency band, which reveals the fact that our planar metamaterial system is electrically excited and the planar structure is hard to couple with the incoming parallel magnetic component in the $xy$ plane. Generally, we notice that the toroidal dipole $\boldsymbol{T}_x$ and the magnetic dipole $\boldsymbol{M}_y$ show considerable scattering contributions at 6.356 and 12.930 GHz, which are near just the two transmission peak frequencies.

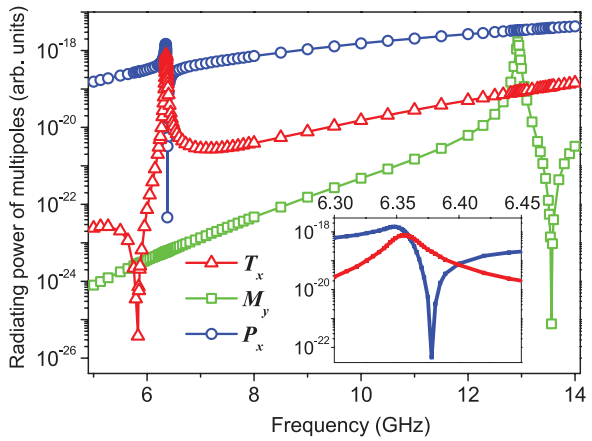


FIG. 5. (Color online) Frequency dependence of radiating power for induced multipoles from the planar toroidal metamaterial: toroidal dipole (red solid curve), magnetic dipole (green dash-dotted curve), and electric dipole (blue dashed curve). The inset illustrates the radiating strength of the toroidal dipole and electric dipole around 6.378 GHz.

Though the $x$ component of the electric dipole moment $\boldsymbol{P}_x$ shows the strongest contribution at the 12.905-GHz transmission peak frequency, the $y$ component of the magnetic dipole moment $\boldsymbol{M}_y$ also provides a significant contribution that can be checked in the time-domain simulated field patterns. While for the 6.378-GHz transmission peak the $x$ component of the toroidal dipole moment $\boldsymbol{T}_x$ plays a dominative role in comparison with the electric and magnetic dipoles, the inset in Fig. 5 clearly illustrates the radiating strength of the toroidal dipole moment $\boldsymbol{T}_x$ and the electric dipole moment $\boldsymbol{P}_x$ around 6.378 GHz. We see that at 6.378 GHz radiating power for the toroidal dipole moment is 3 orders of magnitude larger than that for the electric dipole moment. This is because the electric dipole radiation shows a Fano line-shaped spectrum that comes from radiating interference of the induced current in the trapped mode. All these indicate that the experimentally observed transmission peak at around 6.378 GHz is the toroidal moment response of our planar metamaterial.

## III. CONCLUSIONS

In summary, we demonstrated that a planar metamaterial structure which possesses low-loss and high-$Q$ performance can be constructed with ASRRs due to the excitation of the toroidal dipole and the trapped mode of ASRR. It is shown that a toroidal molecule can be constructed through arrangement of planar ASRRs as meta-atoms via manipulating the structural symmetry of the meta-atoms. The characteristic spectrum is experimentally verified at microwave range. Field maps and multipole moment calculations clearly indicate that the toroidal resonance paves the way for electromagnetic confinement in a subwavelength scale. Although we did our experiments at microwave frequencies, the features of the planar toroidal structure can be generalized to terahertz, infrared, and visible frequencies. Particularly for low-Joule-loss metallic photonic metamaterials, the field localization configuration with a high-$Q$ response and low loss will be beneficial for a myriad of photonic applications in enhancing light-matter interactions.

## ACKNOWLEDGMENTS

This work was supported by NSFC (Grants No. 11174221 and No. 10974144), CNKBRSF (Grant No. 2011CB922001), the National 863 Program of China (Grant No. 2006AA03Z407), NCET (Grant No. 07-0621), STCSM, and SHEDF (Grant No. 06SG24). Work at Ames Laboratory was supported by the US Department of Energy (Basic Energy Sciences, Division of Materials Sciences and Engineering) under Contract No. DE-AC02-07CH11358. Y.F. acknowledges financial support from the China Scholarship Council (No. 201206260055).

## APPENDIX: CALCULATING THE MULTIPOLE MOMENTS

Numerical simulation results shown in Figs. 2–5 were obtained by a homemade brute-force finite-difference-in-time-domain (FDTD)[35] electromagnetic solver (Gallop).[36] In our FDTD simulations, a nonuniform mesh is adopted for accurately describing the geometric information of the structured thin metal layer. Periodic boundary conditions are implemented to portray the realistic situation that our metamaterial slab is a toroidal-molecule array. Along the propagating direction, a Gaussian pulsed plane wave is excited 20 mm away from the planar metamaterial. The electromagnetic fields are recorded on the other side for evaluating the transmission spectra, and the total simulation time is chosen to ensure the field error is below –30 dB. To evaluate the radiating power from the multipoles (as in Fig. 5) we adopted the current density formalization[4,13] by integrating spatial distributed fields over the volume of a planar metamolecule. The radiating power of induced multipole moments (in Fig. 5) has the form

$$I = \frac{2\omega^4}{3c^3}|\boldsymbol{P}|^2 + \frac{2\omega^4}{3c^3}|\boldsymbol{M}|^2 + \frac{2\omega^6}{3c^5}|\boldsymbol{T}|^2 + \cdots, \tag{A1}$$

in which the electric dipole moment is

$$\boldsymbol{P} = \frac{1}{i\omega}\int \boldsymbol{j}\, d^3r, \tag{A2}$$

the magnetic dipole moment is

$$\boldsymbol{M} = \frac{1}{2c}\int (\boldsymbol{r}\times\boldsymbol{j})\, d^3r, \tag{A3}$$

and the toroidal dipole moment is

$$\boldsymbol{T} = \frac{1}{10c}\int \left[(\boldsymbol{r}\cdot\boldsymbol{j})\,\boldsymbol{r} - 2r^2\boldsymbol{j}\right] d^3r, \tag{A4}$$

where $\boldsymbol{j}$ is the current density. We also investigated some other high-order multipoles (e.g., electric quadrupole moments and magnetic quadrupole moments) and found that these three multipoles are mainly contributed components, especially at the toroidal resonant frequencies we are concerned with in this paper.

*boyle429@126.com
†hqlee@tongji.edu.cn
‡soukoulis@ameslab.gov

[1] V. M. Dubovik and V. V. Tugushev, Phys. Rep. **187**, 145 (1990).
[2] Ya. B. Zel'dovich, Sov. Phys. JETP **6**, 1184 (1958).
[3] W. C. Haxton, Science **275**, 1753 (1997).
[4] E. E. Radescu and G. Vaman, Phys. Rev. E **65**, 046609 (2002).
[5] A. Ceulemans, L. F. Chibotaru, and P. W. Fowler, Phys. Rev. Lett. **80**, 1861 (1998).
[6] I. I. Naumov, L. Bellaiche, and H. Fu, Nature (London) **432**, 737 (2004).
[7] C. M. Soukoulis, S. Linden, and M. Wegener, Science **315**, 47 (2007).
[8] C. M. Soukoulis and M. Wegener, Nat. Photonics **5**, 523 (2011).
[9] J. B. Pendry, A. J. Holden, D. J. Robbins, and W. J. Stewart, IEEE Trans. Microwave Theory Tech. **47**, 2075 (1999).
[10] D. Schurig, J. J. Mock, and D. R. Smith, Appl. Phys. Lett. **88**, 041109 (2006).
[11] K. Marinov, A. D. Boardman, V. A. Fedotov, and N. Zheludev, New J. Phys. **9**, 324 (2007).
[12] N. Papasimakis, V. A. Fedotov, K. Marinov, and N. I. Zheludev, Phys. Rev. Lett. **103**, 093901 (2009).
[13] T. Kaelberer, V. A. Fedotov, N. Papasimakis, D. P. Tsai, and N. I. Zheludev, Science **330**, 1510 (2010).
[14] Y. W. Huang, W. T. Chen, P. C. Wu, V. Fedotov, V. Savinov, Y. Z. Ho, Y. F. Chau, N. I. Zheludev, and D. P. Tsai, Opt. Express **20**, 1760 (2012).
[15] D. Sievenpiper, L. Zhang, R. F. Jimenez Broas, N. G. Alexópolous, and E. Yablonovitch, IEEE Trans. Microwave Theory Tech. **47**, 2059 (1999).
[16] N. I. Landy, S. Sajuyigbe, J. J. Mock, D. R. Smith, and W. J. Padilla, Phys. Rev. Lett. **100**, 207402 (2008).
[17] S. Zhang, D. A. Genov, Y. Wang, M. Liu, and X. Zhang, Phys. Rev. Lett. **101**, 047401 (2008).
[18] N. Papasimakis, V. A. Fedotov, N. I. Zheludev, and S. L. Prosvirnin, Phys. Rev. Lett. **101**, 253903 (2008).
[19] N. Liu, T. Weiss, M. Mesch, L. Langguth, U. Eigenthaler, M. Hirscher, C. Sönnichsen, and H. Giessen, Nano Lett. **10**, 1103 (2009).
[20] P. Tassin, L. Zhang, Th. Koschny, E. N. Economou, and C. M. Soukoulis, Phys. Rev. Lett. **102**, 053901 (2009).
[21] C. Kurter, P. Tassin, L. Zhang, Th. Koschny, A. P. Zhuravel, A. V. Ustinov, S. M. Anlage, and C. M. Soukoulis, Phys. Rev. Lett. **107**, 043901 (2011).
[22] T. J. Yen, W. J. Padilla, N. Fang, D. C. Vier, D. R. Smith, J. B. Pendry, D. N. Basov, and X. Zhang, Science **303**, 1494 (2004).
[23] S. Zhang, W. Fan, N. C. Panoiu, K. J. Malloy, R. M. Osgood, and S. R. J. Brueck, Phys. Rev. Lett. **95**, 137404 (2005).
[24] C. Enkrich, M. Wegener, S. Linden, S. Burger, L. Zschiedrich, F. Schmidt, J. F. Zhou, Th. Koschny, and C. M. Soukoulis, Phys. Rev. Lett. **95**, 203901 (2005).
[25] G. Dolling, M. Wegener, C. M. Soukoulis, and S. Linden, Opt. Lett. **32**, 53 (2007).
[26] K. L. Tsakmakidis, A. D. Boardman, and O. Hess, Nature (London) **450**, 397 (2007).
[27] C. M. Soukoulis and M. Wegener, Science **330**, 1633 (2010).
[28] O. Hess, J. B. Pendry, S. A. Maier, R. F. Oulton, J. M. Hamm, and K. L. Tsakmakidis, Nat. Mater. **11**, 573 (2012).
[29] M. Kauranen and A. V. Zayats, Nat. Photonics **6**, 737 (2012).
[30] C. Wu, A. B. Khanikaev, R. Adato, N. Arju, A. A. Yanik, H. Altug, and G. Shvets, Nat. Mater. **11**, 69 (2012).
[31] W. Rechberger, A. Hohenau, A. Leitner, J. R. Krenn, B. Lamprecht, and F. R. Aussenegg, Opt. Commun. **220**, 137 (2003).
[32] E. Prodan, C. Radloff, N. J. Halas, and P. Nordlander, Science **302**, 419 (2003).
[33] N. Liu, H. Liu, S. Zhu, and H. Giessen, Nat. Photonics **3**, 157 (2009).
[34] Y. Fan, J. Han, Z. Wei, C. Wu, Y. Cao, X. Yu, and H. Li, Appl. Phys. Lett. **98**, 151903 (2011).
[35] A. Taflove, *Computational Electrodynamics: The Finite Difference Time Domain Method* (Artech House, Boston, 1995).
[36] Z. Wei, Y. Cao, J. Han, C. Wu, Y. Fan, and H. Li, Appl. Phys. Lett. **97**, 141901 (2010).
[37] V. A. Fedotov, M. Rose, S. L. Prosvirnin, N. Papasimakis, and N. I. Zheludev, Phys. Rev. Lett. **99**, 147401 (2007).
[38] M. I. Stockman, S. V. Faleev, and D. J. Bergman, Phys. Rev. Lett. **87**, 167401 (2001).
[39] U. Fano, Phys. Rev. **124**, 1866 (1961).
[40] B. Luk'yanchuk, N. I. Zheludev, S. A. Maier, N. J. Halas, P. Nordlander, H. Giessen, and C. T. Chong, Nat. Mater. **9**, 707 (2010).
[41] A. E. Miroshnichenko, S. Flach, and Y. S. Kivshar, Rev. Mod. Phys. **82**, 2257 (2010).